

Consequences Of Fully Dressing Quark-Gluon Vertex Function With Two-Point Gluon Lines

Hrayr H. Matevosyan,^{1,2} Anthony W. Thomas,^{2,3} and Peter C. Tandy⁴

¹*Louisiana State University, Department of Physics & Astronomy,
202 Nicholson Hall, Tower Dr., LA 70803, USA*

²*Thomas Jefferson National Accelerator Facility,
12000 Jefferson Ave., Newport News, VA 23606, USA*

³*College of William and Mary, Williamsburg VA 23187, USA*

⁴*Center for Nuclear Research, Department of Physics,
Kent State University, Kent, Ohio 44242, USA*

(Dated: August 5, 2021)

Abstract

We extend recent studies of the effects of quark-gluon vertex dressing upon the solutions of the Dyson-Schwinger equation for the quark propagator. A momentum delta function is used to represent the dominant infrared strength of the effective gluon propagator so that the resulting integral equations become algebraic. The quark-gluon vertex is constructed from the complete set of diagrams involving only 2-point gluon lines. The additional diagrams, including those with crossed gluon lines, are shown to make an important contribution to the DSE solutions for the quark propagator, because of their large color factors and the rapid growth in their number.

PACS numbers: 12.38.Aw; 11.30.Rd; 12.38.Lg; 12.40.Yx

Notice: Authored by Jefferson Science Associates, LLC under U.S. DOE Contract No. DE-AC05-06OR23177. The U.S. Government retains a non-exclusive, paid-up, irrevocable, world-wide license to publish or reproduce this manuscript for U.S. Government purposes.

I. INTRODUCTION

In recent years there has been significant progress in the study of the spectrum of hadrons, as well as their non-perturbative structure and form factors, through approaches that are manifestly covariant and which accommodate both dynamical chiral symmetry breaking (DCSB) and quark confinement [1]. Covariance provides efficient and unambiguous access to form factors [2, 3, 4] and parton distribution functions [5]. The covariant approach to modeling QCD with which we will be concerned is based upon the Dyson-Schwinger equations (DSE) of QCD [1]. These are coupled integral equations of motion for the QCD Green's functions or n-point functions. The DSE for any particular n-point function involves higher (n+1)-point functions and so on. One needs to employ a truncation of the coupled equations for practical calculations.

One of the simplest and most studied DSEs is the quark propagator DSE, the quark gap equation

$$S^{-1}(p) = Z_2 S_0^{-1}(p) + C_F Z_1 \int_q^\Lambda g^2 D_{\mu\nu}(p-q) \gamma_\mu \times S(q) \Gamma_\nu(q,p), \quad (1)$$

where $S_0^{-1}(p) = i\gamma \cdot p + m_{bm}$, m_{bm} is the bare current quark mass, $\Gamma_\nu(q,p)$ is the dressed quark-gluon vertex function, $\int_q^\Lambda = \int^\Lambda d^4q/(2\pi)^4$ denotes a loop integral regularized in a translationally-invariant manner at mass-scale Λ . Here $Z_1(\mu^2, \Lambda^2)$ is the vertex renormalization constant to ensure $\Gamma_\sigma = \gamma_\sigma$ at the renormalization scale μ and $Z_2(\mu^2, \Lambda^2)$ is the quark wave function renormalization constant. The color factor in Eq. (1) is $C_F = (N_c^2 - 1)/2N_c$.

The general form for $S(p)^{-1}$ is

$$S(p)^{-1} = i\gamma \cdot p A(p^2, \mu^2) + B(p^2, \mu^2) \quad (2)$$

and the renormalization condition at scale $p^2 = \mu^2$ is $S(p)^{-1} \rightarrow i\gamma \cdot p + m(\mu)$, where $m(\mu)$ is the renormalized current quark mass. One can see from Eq. (1) that, in principle, one must first solve the DSE for the gluon 2-point function as well as the DSE for the dressed quark-gluon vertex. In the renormalization group improved rainbow approximation [6], one replaces the combination of those two objects by bare vertex times an effective gluon 2-point function. The latter has a phenomenological infrared part that joins smoothly to the 1-loop renormalization group result for the ultraviolet running coupling. Typically one infrared parameter is sufficient to generate the empirical value of the quark condensate. When the

same kernel and dressed propagators are used for the Bethe-Salpeter equation (BSE), this ladder-rainbow (LR) model gives a very good account of light quark vector and pseudoscalar ground state mesons [7] and many other observables – see Ref. [1] for a review.

As this LR truncation is a non-perturbative truncation, one does not have an easy handle on its accuracy. Recent efforts have been made to perform calculations of meson masses beyond ladder-rainbow truncation [8, 9, 10]. These studies employ a quark-gluon vertex that is dressed by certain classes of diagrams constructed from 2-point gluon functions alone. The results of a truncation back to a bare vertex indicate that the error in the LR truncation is typically 10-30 percent, depending on the class of vertex diagram that is taken into account. To make such calculations feasible, the gluon propagator is simplified to a momentum delta function so that non-linear integral equations are reduced to non-linear algebraic equations. The sum of ladder-rainbow diagrams for the vertex was implemented in Ref. [8], while in Ref. [9] the important attractive effects of dressing with 3-point gluon functions were added phenomenologically. The 4-point gluon functions have so far been neglected altogether. In our previous work [10], we studied an improved ladder-rainbow summation in which internal vertices were self-consistently dressed. In the current work we explore a scheme for including all possible diagrams involving vertex dressing with 2-point gluon functions and explore the effects of this generalization on the behavior of the quark propagator amplitudes. This entails the inclusion of crossed gluon line diagrams. A study of fully dressed quark-gluon vertex in scalar $\varphi^2\chi$ theory with Munczek-Nemirowski gluon propagator of Ref. [11] showed that the solutions for quark propagator functions show large variations in the region of the small momenta in comparison with those corresponding to LR truncation of the quark DSE.

To demonstrate the relevance of the current dressing scheme, consider the vertex with exactly 2 gluon lines, Fig. 1. In our previous work with the most general vertex dressing scheme to date [10], we extended the ladder-summed approximation of Refs. [8, 9] (Fig. 1a) to self-consistently include the dressing of internal vertices (Figs. 1b and 1c). The same procedure was extended to a general number of gluon lines and the contributions were summed until convergence was reached for this improved ladder-rainbow sum. Crossed gluon line diagrams, such as Fig. 1d were not included. Convergence in this improved ladder-rainbow sum was found in the vertex itself, in the quark DSE solutions, and in the pseudoscalar and vector meson masses.

The diagrams in the improved ladder-rainbow sum have the same simple color structure and the associated color factors are powers of one basic color factor. The color structure analysis of the diagrams omitted from the improved ladder-rainbow class shows that they can have significantly larger color-factors and that, at the very least, their role should be explored. For example, with N_c colors, the color factor associated with Figs. 1a, 1b and 1c are $1/(2N_c)^2$, whereas for the crossed gluon diagram of Fig. 1d the color factor is $(N_c^2 + 1)/(2N_c)^2$. In general, similar examples occur at higher order. Also working to magnify the contributions to the vertex from many gluon lines is the fact that the number of such diagrams increases rapidly. A formal analysis of these additional diagrams in terms of $1/N_c$ expansion is presented in Ref. [12].

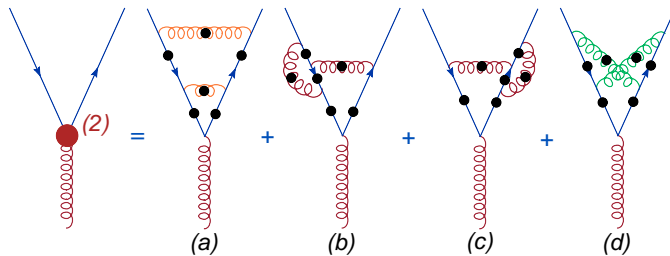


FIG. 1: (Color Online) Quark-gluon vertex diagrams at $\mathcal{O}(g^5)$, neglecting 3-gluon and 4-gluon coupling. The large red circle denotes the second order vertex and the small black circles indicate dressed propagators. Diagram (a) is part of the ladder sum [8, 9], while diagrams (b) and (c) are added in the improved ladder sum [10], and diagram (d) enters in the extension considered in this work. Crossed gluon diagrams, such as (d), prove to be important because of their significantly larger color factors.

II. THE FULLY DRESSED VERTEX WITH TWO-POINT GLUON LINES

We employ Landau gauge and a Euclidean metric, with: $\{\gamma_\mu, \gamma_\nu\} = 2\delta_{\mu\nu}$; $\gamma_\mu^\dagger = \gamma_\mu$; and $a \cdot b = \sum_{i=1}^4 a_i b_i$. The dressed quark-gluon vertex for gluon momentum k and quark momentum p can be written $ig t^c \Gamma_\sigma(p+k, p)$, where $t^c = \lambda^c/2$ and λ^c is an SU(3) color matrix. In general, $\Gamma_\sigma(p+k, p)$ has 12 independent invariant amplitudes. We are particularly concerned in this work with the vertex at $k=0$, in which case the general form is

$$\Gamma_\sigma(p) = \alpha_1(p^2)\gamma_\sigma + \alpha_2(p^2)\gamma \cdot p p_\sigma - \alpha_3(p^2)ip_\sigma + \alpha_4(p^2)i\gamma_\sigma \gamma \cdot p \quad (3)$$

where $\alpha_i(p^2)$ are invariant amplitudes.

We propose a scheme for dressing the vertex function that includes all possible contributions constructed with two-point gluon lines up to n gluon lines. We can decompose the vertex function into a sum of all contributions with exactly i gluon lines:

$$\Gamma_\mu = \sum_{i=0} \Gamma_\mu^i, \quad (4)$$

where $\Gamma_\mu^0 = Z_1 \gamma_\mu$.

In previous work we developed a scheme to include all vertex diagrams that have a ladder structure but further improved it by the self-consistent dressing of all internal vertices [10]. In that case the contribution Γ_μ^i is generated from three vertex contributions having a smaller number of gluon lines by adding one gluon ladder rung with dressed vertices. If the number of gluon lines in the three vertex contributions are denoted j, k and l , then summation is made over j, k and l such that $j + k + l + 1 = i$. That iterative self-consistent ladder scheme is described by

$$\begin{aligned} \Gamma_\mu^i(p + k, p) = & - \left(-\frac{1}{2N_c} \right) \sum_{\substack{j,k,l \\ i=j+k+l+1}} \int_q^\Lambda g^2 D_{\sigma\nu}(p - q) \\ & \times \Gamma_\sigma^j(p + k, q + k) S(q + k) \Gamma_\mu^l(q + k, q) S(q) \Gamma_\nu^k(q, p), \quad (5) \end{aligned}$$

for $i \geq 1$. Here, and in all vertex constructions that we discuss and implement, the quark propagators that are internal to the vertex are self-consistently dressed using the gap equation, Eq. (1), with the dressed vertex at the order being discussed. The color factors of all contributions included in this improved ladder vertex are correctly generated by the iterations of $-\frac{1}{2N_c}$ implied by the above. Such a vertex, generated by 2-point gluon lines, is repulsive and as a consequence one finds [9] that the dominant vertex amplitude $\alpha_1(p^2) < 1$.

However, the available lattice data indicate that $\alpha_1(p^2) > 1$ much as it is in an Abelian theory. Certainly in the ultraviolet, where a one-loop analysis is reliable [13], $\alpha_1(p^2) \rightarrow 1$ from above because of the strong attraction is provided by the 3-gluon coupling term with its dominant and large color factor $+\frac{N_c}{2}$. In Refs. [9, 10], it was argued that an effective way to simulate such physics in studies like the present is to assume the momentum dependence of the corresponding 3-gluon coupling contribution to the vertex is similar enough to Eq. (5) to allow the color factor there to be replaced by the sum of the two, which is C_F , the color factor of the quark DSE in Eq. (1). To reproduce lattice vertex data, and to explore the effect

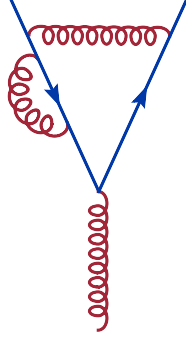


FIG. 2: (Color Online) Quark self-energy type contribution in dressing the quark-gluon vertex.

of 3-gluon coupling in a slightly more general way, Refs. [9, 10], employed Eq. (5) with color factor $\mathcal{C}C_F$ where \mathcal{C} varies in the range $-\frac{1}{2N_c C_F}$ to 1. Here we will initially use the lower limit which corresponds to omitting all consideration of 3-gluon coupling. Subsequently, with the choice $\mathcal{C} = 0.5$, we explore the likely influence of 3-gluon coupling with the present vertex.

In this present work we explore the addition of the remaining class of vertex diagrams that are beyond those in the improved ladder sum outlined above, but still obtainable in terms of 2-point gluon functions.

To generate such a vertex, we use a recursive algorithm for obtaining all the contributions with exactly i gluon lines, Γ_μ^i , from the diagrams contributing to Γ_μ^{i-1} . We take each diagram contributing to Γ_μ^{i-1} and consider the diagrams produced by making all possible insertions of a single gluon line so that it starts and ends on a fermion line without being simply a fermion self-energy insertion (see Fig. (2)). Then, to avoid double counting, a check is made as to whether the resulting diagram was already produced from any previous construction at the same order. One can easily see that the algorithm works for constructing the one-loop diagram from the bare vertex and from that the two-loop diagrams of Fig. (1). The steps of the algorithm are illustrated in Fig. (3).

It is trivial to prove, using mathematical induction, that this algorithm produces *all* possible diagrams involving n gluon lines in dressing the vertex for any $n \geq 1$. In the previous paragraph we demonstrated that all the first and second order diagrams are generated using this algorithm. Let us suppose, for some $n > 1$, that we start with the correct diagrammatic content of Γ_μ^{n-1} but that the algorithm for Γ_μ^n failed to produce a certain valid diagram with n gluon lines. It is easy to see that we can always find one gluon line, which can be

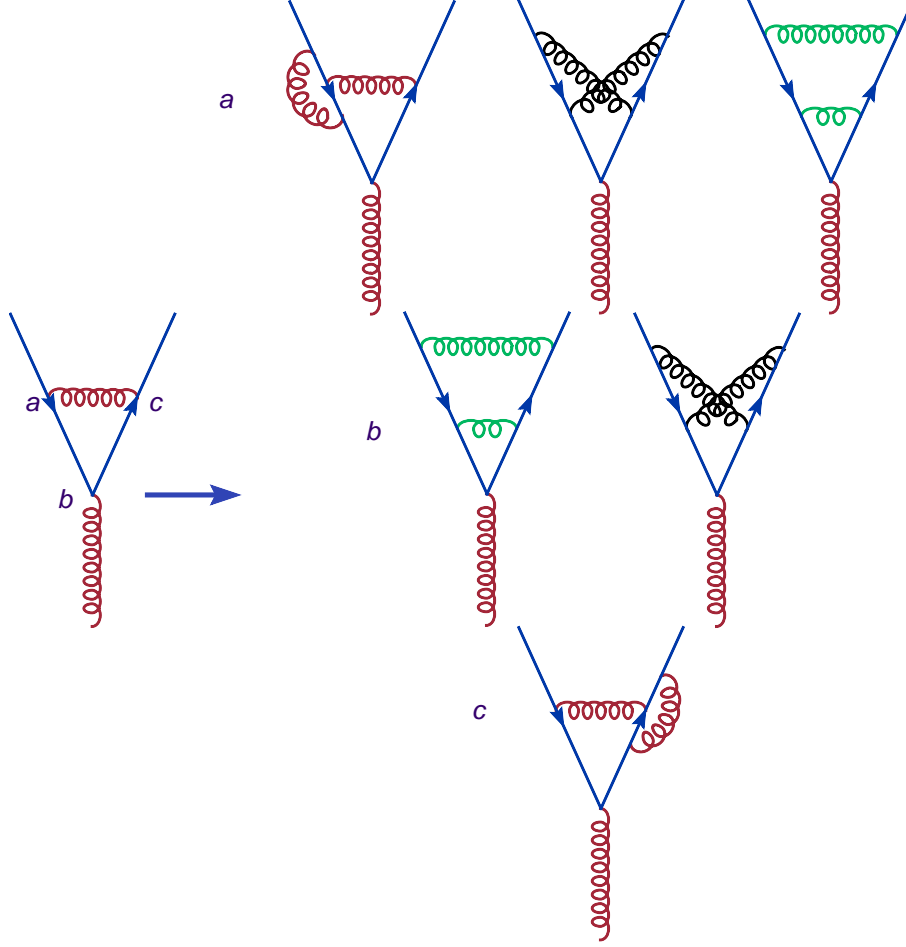


FIG. 3: (Color Online) Generating all the second order diagrams from the only first order diagram by making all possible insertions of a single gluon line into the first order vertex diagram. The letters indicate the starting point of the inserted line. We note that there are several redundant diagrams generated, which must be removed.

removed from that diagram so that the remaining $n - 1$ gluon lines are not simply quark self-energy insertions. Hence the produced parent vertex is a valid member of Γ_μ^{n-1} and the supposition that all possible insertions into it are not capable of generating all members of Γ_μ^n is incorrect.

In fact, the gluon line that can be removed is easy to find in a diagram. If a gluon line attached to the end of a quark line cannot be so removed, then the other end of this gluon line separates ends of a second gluon line that would otherwise be a self-energy insertion. This second gluon line is the one that can be removed.

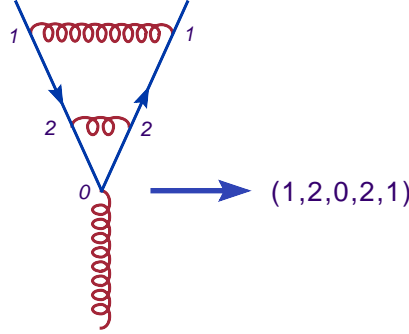


FIG. 4: (Color Online) Constructing the set of numbers uniquely identifying one of the second order diagrams.

$$\left(\begin{array}{cccccccc} & & & & n & n & & \\ & & & & \swarrow & \searrow & & \\ 1, & 2, & 1, & \dots, & 0, & \dots, & n-5, & n-1 \end{array} \right)$$

FIG. 5: (Color Online) The sets representing all diagrams with exactly n gluon lines are obtained from those corresponding to diagrams with exactly $n - 1$ lines by inserting a pair of n 's into the set and making all possible permutations, so they are never next to each other.

The algorithm described above is easy to implement in practice by constructing a set of numbers uniquely identifying each diagram. We build the set by enumerating the bare quark-gluon vertices in a diagram with $n - 1$ gluon lines from 1 to $n - 1$ and assigning the same numbers to the vertices attached to the same gluon propagators. We assign 0 to the external gluon vertex. An example of such construction is shown in Fig. (4).

To construct the vertices with n gluon lines we insert a pair of integers n into the set described above, so that they are not next to each other, as illustrated in Fig. (5). We relabel the resulting set in ascending order and check whether the final set was already generated.

1. Algebraic Analysis

In order to solve the gap equation with our dressed quark-gluon vertex one needs the gluon 2-point function. As in the previous studies of this kind, we again employ the Munczek-

Nemirovsky Ansatz [14] for the interaction kernel in the form

$$g^2 D_{\mu\nu}(k) \rightarrow \left(\delta_{\mu\nu} - \frac{k_\mu k_\nu}{k^2} \right) (2\pi)^4 \mathcal{G}^2 \delta^4(k), \quad (6)$$

where the parameter \mathcal{G}^2 is a measure of the integrated kernel strength. This simplification reduces the multi-dimensional integral equations for the vertex and the dressed quark propagator to algebraic ones that make the analysis feasible.

The algebraic form of the gap equation for the quark propagator corresponding to the gluon propagator in Eq. (6) is

$$S^{-1}(p) = i\gamma \cdot p + m_{bm} + \mathcal{G}^2 \gamma_\mu S(p) \Gamma_\mu(p). \quad (7)$$

After projection onto the two Dirac amplitudes we have

$$A(p^2) = 1 - \mathcal{G}^2 \frac{i}{4} \text{tr} \left[\frac{\gamma \cdot p}{p^2} \gamma_\mu S(p) \Gamma_\mu(p) \right], \quad (8)$$

$$B(p^2) = m_{bm} + \mathcal{G}^2 \frac{1}{4} \text{tr} [\gamma_\mu S(p) \Gamma_\mu(p)]. \quad (9)$$

Equations (8) and (9) are solved simultaneously with a vertex function calculated at a specified order n of vertex dressing.

The calculations of the Dirac algebra for the vertex diagrams was performed using computer-algebraic methods provided by the *FeynCalc* package [15] for *Mathematica* [16]. The color factors were calculated by numerical contraction of the SU(3) color matrices. The number of possible diagrams grows extremely fast with the number of gluon lines included, making it difficult to advance too far with the number of loops. For example, while there are only 4 possible diagrams with exactly 2 internal gluon lines, there are 27 with 3 and 38,232 with 6 internal lines. Such a rapid increase in the number of possible contributions forced us to use parallel computing to calculate the invariant amplitude functions for the vertex with exactly 6 gluon lines within a reasonable time frame. The contributions to Γ_μ^7 include more than 5×10^5 possible diagrams, which we did not consider feasible to calculate. The comparison of the number of diagrams with the previous dressing schemes is shown in Table I.

The numerical solutions of the gap equation constructed with the full vertex are shown in Figs. 6 and 7 for a current quark mass $m = 17$ MeV. No attempt has been made to simulate 3-gluon coupling – i.e., the color factors used are as directly given by the $SU(3)_c$

TABLE I: Comparison of the number of diagrams with exactly n gluon lines included in various vertex dressing schemes: ladder rainbow summed [8, 9], self-consistently improved ladder rainbow summed [10], and the present full vertex obtainable with just 2-point gluon lines.

n	<i>LRSummed</i>	<i>Improved</i>	<i>Full</i>
2	1	3	4
3	1	6	27
6	1	21	38, 232
7	1	28	$\sim 5 * 10^5$

algebra. As found in previous analysis with this model, the results for even and odd n behave differently. The even orders provide a behavior for $A(s)$ and $M(s)$ that is analytic and well-defined in the infrared spacelike region continuing into the timelike region $s > -1$ explored here. Mass generation is strong and investigations of the approach to the chiral limit $m \rightarrow 0$ indicate that these solutions are continuously connected to the Nambu-Goldstone mode of spontaneous breaking of chiral symmetry.

The odd n solutions $n \geq 3$ develop non-analytic points in the infrared. There is also a tendency for significantly weaker mass generation in such solutions. Evidently, repulsive color factors dominate for odd n more than for even n and the mass generation effects are in accord with that.

There is no convincing evidence of convergence with respect to increasing n . At least two factors are at work here. Firstly, with the increasing number n of gluon lines, there are diagrams at each order that have color factors that are comparable to that of the $n = 1$ contribution to the vertex. The class of diagrams omitted in previous studies of this type, e.g., Fig. 1d, contains members that have larger color factors than the improved ladder-rainbow class. Secondly, the number of diagrams specified by n increases rapidly with n , as illustrated in Table I.

2. Effect of 3-point gluon function dressing

Explicit calculations with gluon 3-point functions proved to be extremely difficult, both from the point of view of reproducing all possible diagrams at some non-trivial order in quark-gluon coupling and from the fact that no suitable, model gluon 2-point function is

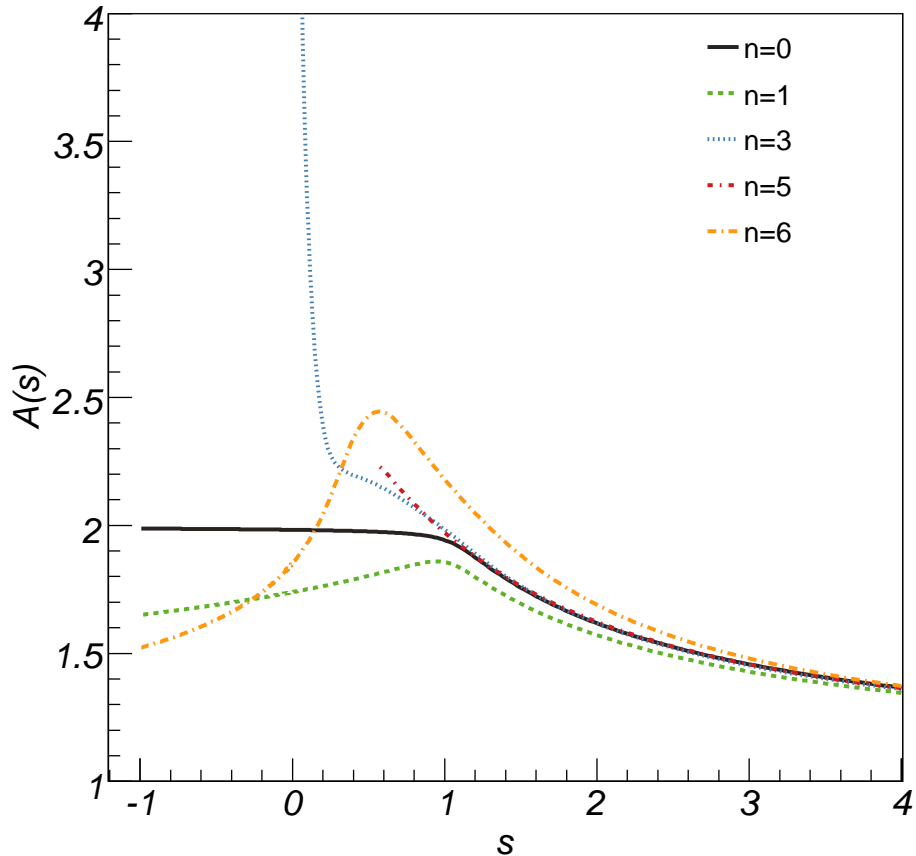


FIG. 6: (Color Online) Quark propagator amplitude $A(s)$ versus Euclidean $s = p^2$. We use the interaction mass scale $\mathcal{G} = 1$ GeV and the current mass is $m = 0.0175 \mathcal{G} = 17.5$ MeV. We show the influence of vertex dressing to order n in the number of gluon lines as described in the text. $n = 0$ yields the solid curve and the result is the ladder-rainbow truncation. The other curves are $n = 1$ (long dashed curve, 1-loop vertex), $n = 3$ (short dashed curve), $n = 5$ (dot short dashed curve) and $n = 6$ (dot long dashed curve).

known to us which would allow for feasible calculations beyond one or two loops. Hence we resort to the method introduced in Ref. [9], which allows one to effectively account for 3-point gluon function dressing of the vertex through the introduction of the phenomenological parameter \mathcal{C} , which for $N_c = 3$ can take values in the range $-1/8 \leq \mathcal{C} \leq 1$, as discussed after Eq. (5).

We chose to implement this phenomenological scheme only for the sub-class of vertex

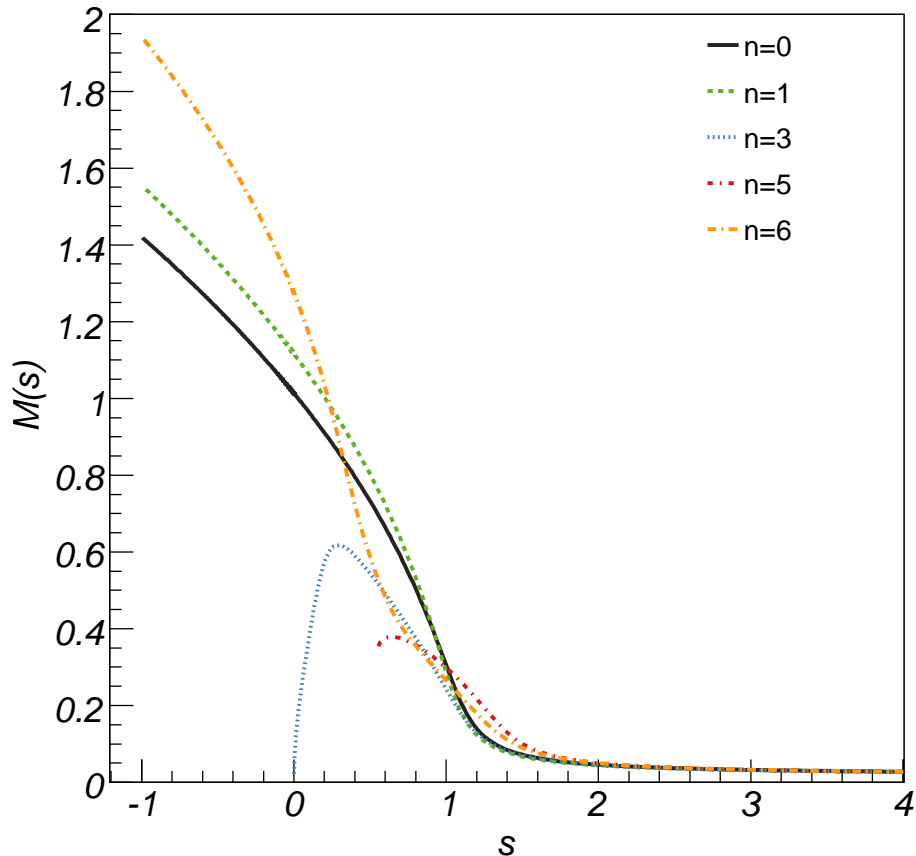


FIG. 7: (Color Online) Quark mass function $M(s)$ versus Euclidean $s = p^2$. We use the interaction mass scale $\mathcal{G} = 1$ GeV and the current mass is $m = 0.0175 \mathcal{G} = 17.5$ MeV. We show the influence of vertex dressing to order n in the number of gluon lines as described in the text. $n = 0$ yields the solid curve and the result is the ladder-rainbow truncation. The other curves are $n = 1$ (long dashed curve, 1-loop vertex), $n = 3$ (short dashed curve), $n = 5$ (dot short dashed curve) and $n = 6$ (dot long dashed curve).

diagrams that correspond to the improved ladder structure where its motivation is unambiguous. We note that all such diagrams have the same color factors as illustrated in Eq. (5). The results show that for the parameter range $\mathcal{C} \in (0.375, 0.8)$ the solutions of the gap equation have significant mass generation even for the odd n values. This is indicative of the attractive effect of the 3-gluon coupling mechanism. Also, in this circumstance there is a much weaker tendency of the odd orders $n \geq 3$ to develop non-analytic points in the deep

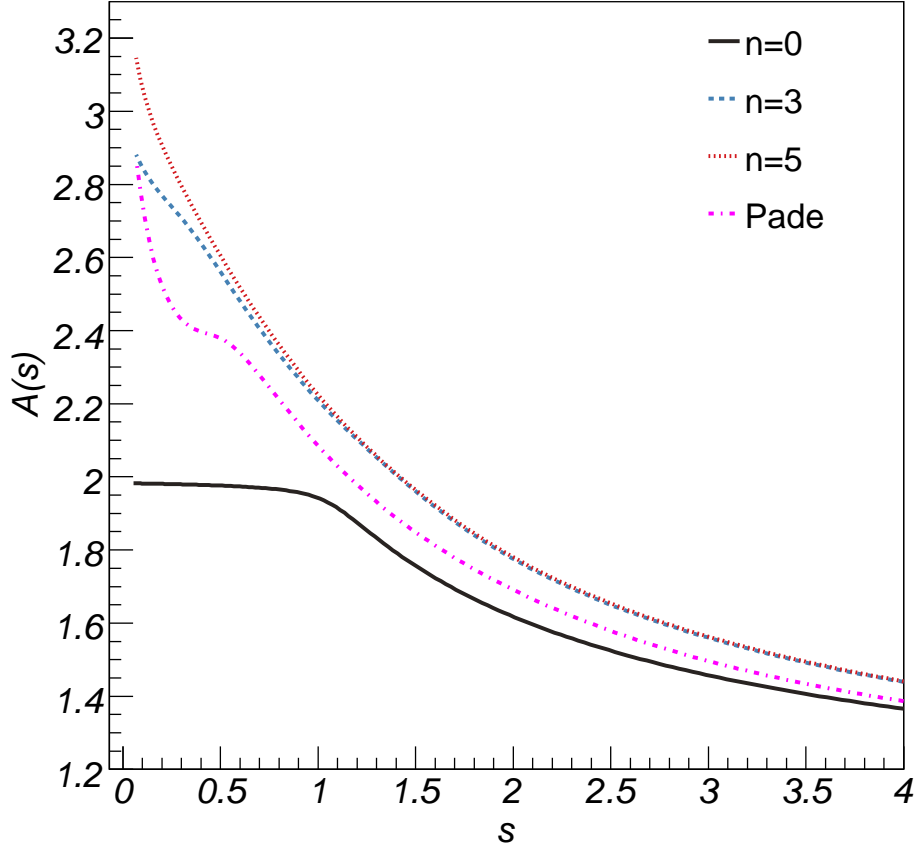


FIG. 8: (Color Online) Quark propagator amplitude $A(s)$ versus Euclidean $s = p^2$. We use the interaction mass scale $\mathcal{G} = 1$ GeV, the current mass is $m = 0.0175 \mathcal{G} = 17.5$ MeV. Partial account has been taken of 3-gluon coupling through the parameter $\mathcal{C} = 0.5$ which induces more mass generation. The influence of quark-gluon vertex dressing to order n in the number of gluon lines: $n = 0$ (solid curve, ladder rainbow truncation), $n = 3$ (long dashed curve), and $n = 5$ (short dashed curve). The dot dashed curve shows the Padé approximation to the vertex.

infrared. The solutions for $\mathcal{C} = 0.5$ are presented in Figs. 8 and 9.

3. Padé Approximant

One can see from Figs. (8) and (9) that even with the enhanced mass generation generated by the strong attractive role of the effective 3-point gluon coupling, the solutions do not show

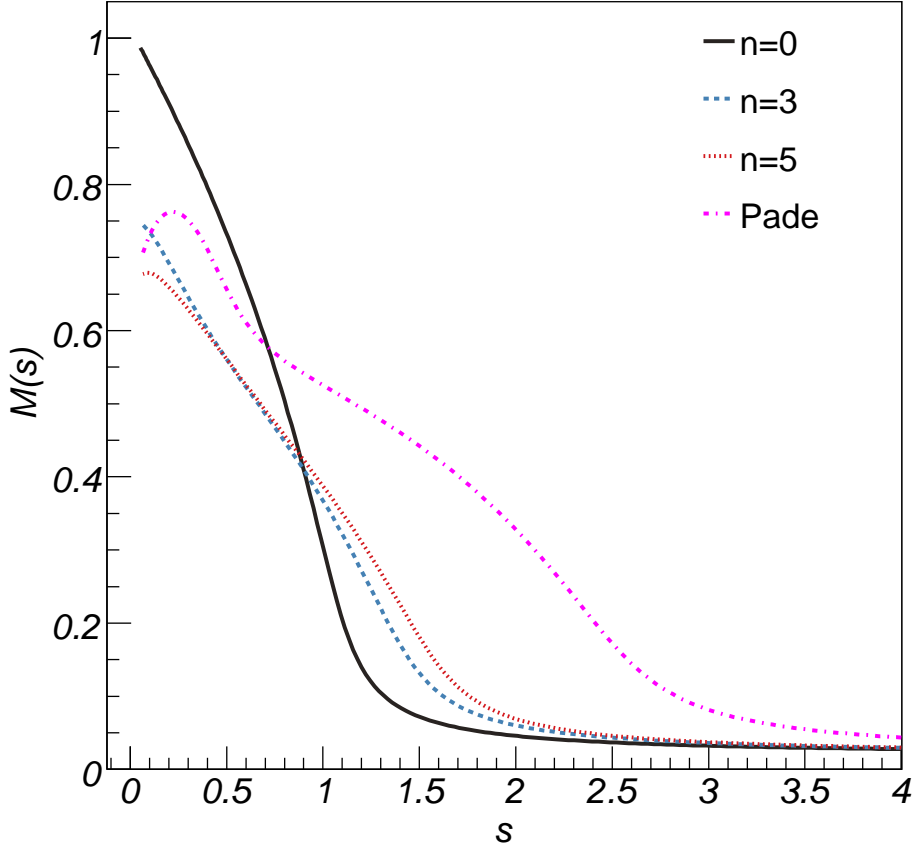


FIG. 9: (Color Online) Quark propagator amplitude $M(s)$ versus Euclidean $s = p^2$. We use the interaction mass scale $\mathcal{G} = 1$ GeV, the current mass is $m = 0.0175 \mathcal{G} = 17.5$ MeV. Partial account has been taken of 3-gluon coupling through the parameter $\mathcal{C} = 0.5$ which induces more mass generation. The influence of quark-gluon vertex dressing to order n in the number of gluon lines: $n = 0$ (solid curve, ladder rainbow truncation), $n = 3$ (long dashed curve), and $n = 5$ (short dashed curve). The dot dashed curve shows the Padé approximation to the vertex.

convincing convergence with respect to the maximum number, n , of gluon lines allowed in the quark-gluon vertex dressing, even in the space-like region. To seek more reliable information, we employ a Padé approximant to re-sum the quark self-energy contributions with respect to n . While the details of this calculation are presented in Appendix A, the graphs corresponding to the solutions of the gap equation with Padé approximant used for the quark self-energy contribution are shown in magenta in Figs. (8) and (9). It is clear from

the graph that our results are significantly different from those obtained using LR truncation and illustrate that convergence is still remote for $n \approx 5$.

Unfortunately the present model does not allow consistent solutions in the time-like region, where the propagators are needed in order to calculate the meson masses by solving the corresponding Bethe-Salpeter equations.

III. SUMMARY

We have extended recent studies of the effects of quark-gluon vertex dressing upon the solutions of the Dyson-Schwinger equation for the quark propagator. The approach we have followed uses a momentum delta function to represent the dominant infrared strength of the effective gluon propagator so that the resulting integral equations become algebraic. When the quark-gluon vertex is constructed from diagrams that involve only 2-point gluon lines, the algebraic form allows the summation of all vertex diagrams, self-consistently with solution of the quark propagator. Previous studies along these lines have treated the ladder-rainbow class of vertex diagram, and subsequently an improved ladder-rainbow class in which all internal vertices are self-consistently dressed. Whereas the earlier improvements showed only minor differences from the Ladder-Rainbow approximation, the inclusion of all two gluon lines at a given order leads to much larger corrections in the infrared space-like as well as the time-like region.

As far as we are able to take the calculations, there is no evident convergence with increasing n . In particular, the behavior with n even or odd is rather different. At least two factors are at work here. Firstly, with increasing n , there are diagrams at each order that have color factors which are comparable with that of the $n = 1$ contribution to the vertex. The class of diagrams omitted in previous studies of this type, contains members that have larger color factors than the improved ladder-rainbow class of diagrams. Secondly, the number of diagrams that must be included increases rapidly with n .

The resulting solutions of the gap equation with the corresponding vertex calculated up to a given order, n , in gluon lines show significant deviation from those calculated previously using either a bare vertex or a vertex dressed according to a ladder-rainbow sum or its self-consistent improvement. The investigation of the infrared behavior of the ghost and gluon n -point functions of Refs. [17, 18] indicate that the contributions of ghost loops in dressing

the quark-gluon vertex are dominant. It is possible that a consistent treatment involving 2-, 3-, and 4-point gluon functions as well as ghost contributions might enable a convergent summation of diagrams for the vertex. However the present simplified gluon propagator permits only zero momentum and this is not compatible with an explicit treatment of ghost 2-point, and 3- and 4-point gluon functions. In spite of the the numerous interesting applications of the Munczek-Nemirovsky model, it is also possible that the advantages of the simple gluon propagator, in allowing algebraic simplification of the summation of vertex diagrams within the quark DSE , are outweighed by model artifacts. It would be very important to explore ways to repeat this calculation with a more realistic gluon propagator.

Acknowledgments

This work was supported in part by DOE contract DE-AC05-06OR23177, under which Jefferson Science Associates, LLC, operates Jefferson Lab, the U.S. National Science Foundation under Grant Nos. PHY-0500291 and PHY-0610129 and the Southeastern Universities Research Association(SURA). HHM thanks Jerry P. Draayer for his support during the course of the work, the Graduate School of Louisiana State University for a fellowship partially supporting his research, George S. Pogosyan and Sergue I. Vinitzky for their support at the Joint Institute of Nuclear Research.

APPENDIX A: PADÉ APPROXIMANT FOR THE QUARK SELF-ENERGY

The solutions of the gap equation (7) for the quark propagator amplitudes $A(s)$ and $B(s)$ depend on the number n of the included gluon lines in the calculations through the Dirac projections of the quark self-energy term with appropriately dressed quark-gluon vertex function on the RHS of Eqs.(8) and (9) (the terms under the tr). We re-summed the perturbative solutions of the gap equation and obtained a solution at $n = \infty$ by employing a Padé approximant in n for these self-energy terms.

In order to construct a Padé approximant for each of these terms we established their dependence on n by introducing a fictitious coefficient, ω , to the bare quark-gluon vertex coupling g in dressing the vertex function and constructing the projections of the self-energy

term in Eqs. (8) and (9). In each case a Padé approximant of the following form

$$f(\lambda) = \frac{a_0 + a_1\lambda + a_2\lambda^2}{1 + b_1\lambda + b_2\lambda^2}, \quad (\text{A1})$$

where $\lambda = \omega^2$, was used to match the appropriate self-energy projection term by solving for the coefficients a_i and b_i . We considered the self-energy projection terms with the quark-gluon vertex dressed to order $n = 3$ in the number of gluon loops to determine all the parameters in (A1).

After determining the coefficients a_i and b_i , the parameter ω was set to 1 and the corresponding coupled equations for $A(s)$ and $B(s)$ were solved. For the case $\mathcal{C} = 0.5$, the solutions obtained with the approximant self-energy projection terms are finite and continuous in the space-like region.

-
- [1] P. Maris and C. D. Roberts, *Int. J. Mod. Phys.* **E12**, 297 (2003), nucl-th/0301049.
 - [2] J. Volmer et al. (The Jefferson Lab F(pi) Collaboration), *Phys. Rev. Lett.* **86**, 1713 (2001), nucl-ex/0010009.
 - [3] P. Maris and P. C. Tandy, *Phys. Rev.* **C62**, 055204 (2000), nucl-th/0005015.
 - [4] R. Alkofer, A. Holl, M. Kloker, A. Krassnigg, and C. D. Roberts, *Few Body Syst.* **37**, 1 (2005), nucl-th/0412046.
 - [5] I. C. Cloet, W. Bentz, and A. W. Thomas, *Phys. Lett.* **B621**, 246 (2005), hep-ph/0504229.
 - [6] P. Maris and C. D. Roberts, *Phys. Rev.* **C56**, 3369 (1997), nucl-th/9708029.
 - [7] P. Maris and P. C. Tandy, *Phys. Rev.* **C60**, 055214 (1999), nucl-th/9905056.
 - [8] A. Bender, W. Detmold, C. D. Roberts, and A. W. Thomas, *Phys. Rev.* **C65**, 065203 (2002), nucl-th/0202082.
 - [9] M. S. Bhagwat, A. Holl, A. Krassnigg, C. D. Roberts, and P. C. Tandy, *Phys. Rev.* **C70**, 035205 (2004), nucl-th/0403012.
 - [10] H. H. Matevosyan, A. W. Thomas, and P. C. Tandy, *Phys. Rev.* **C75**, 045201 (2007), nucl-th/0605057.
 - [11] W. Detmold, *Phys. Rev.* **D67**, 085011 (2003), hep-ph/0301007.
 - [12] H. H. Matevosyan and A. W. Thomas (2007), arXiv:0708.1019 [hep-ph].
 - [13] M. S. Bhagwat and P. C. Tandy, *Phys. Rev.* **D70**, 094039 (2004), hep-ph/0407163.

- [14] H. J. Munczek and A. M. Nemirovsky, Phys. Rev. **D28**, 181 (1983).
- [15] R. Mertig, M. Bohm, and A. Denner, Comput. Phys. Commun. **64**, 345 (1991), URL <http://www.feyncalc.org>.
- [16] Wolfram, Mathematica 5.2 (2005), URL <http://www.wolfram.com>.
- [17] R. Alkofer, C. S. Fischer, and F. J. Llanes-Estrada, Phys. Lett. **B611**, 279 (2005), hep-th/0412330.
- [18] R. Alkofer, C. S. Fischer, and F. J. Llanes-Estrada (2006), hep-ph/0607293.